

A note on in situ estimates of sorption using push-pull tests

Giorgio Cassiani

Dipartimento di Scienze Geologiche e Geotecnologie, Università di Milano-Bicocca, Milan, Italy

Lee F. Burbery

Department of Environmental Science, Lancaster University, Lancaster, UK

Michela Giustiniani

Dipartimento di Ingegneria Civile ed Ambientale, Sezione Georisorse e Ambiente, Università di Trieste, Trieste, Italy

Received 31 May 2004; revised 15 November 2004; accepted 13 December 2004; published 5 March 2005.

[1] A sensitivity analysis reveals that large uncertainty exists in estimates of solute retardation factor R made from sorption push-pull tests. A simplified push-pull data interpretation method for estimating instantaneous linear sorption in confined aquifers is developed. The new method is less restrictive in its application than the conventional method that uses an approximate analytical solution to the push-pull test problem.

Citation: Cassiani, G., L. F. Burbery, and M. Giustiniani (2005), A note on in situ estimates of sorption using push-pull tests, *Water Resour. Res.*, 41, W03005, doi:10.1029/2004WR003382.

1. Introduction

[2] The need to characterize the behavior of reactive solutes in the subsurface, together with the practical and financial limitations of large-scale tracer tests, has motivated the development of fast, single-well tracer tests, such as the push-pull test. Recently, a simplified model has been proposed for the interpretation of push-pull tests applied to determine solute retardation properties [Schroth *et al.*, 2001]. The method is based on the approximate analytical solution of the radial dispersion problem presented by Gelhar and Collins [1971], which by default limits the applicability of the method to cases where the distance traveled by the solute is much larger than the aquifer longitudinal dispersivity. In the proposed interpretation method the aquifer longitudinal dispersivity is estimated from the breakthrough curve of a nonsorbing tracer, and the retardation factor is consequently estimated from the breakthrough curve of an adsorbing solute, using the same dispersivity value. The sensitivity of the parameters and interrelationship that exists between them are as yet uncharacterized.

[3] The objectives of this technical note are (1) to investigate the sensitivity of, and assess any correlation that may exist between, the two estimated governing parameters of push-pull sorption studies: dispersivity and retardation factor, by means of a numerical radial-flow model and automated numerical inversion procedure; (2) to compare results obtained with the numerical model with those calculated using the Gelhar and Collins [1971] model to highlight the limitations of the existing interpretation method [Schroth *et al.*, 2001] that is heavily based on this model; and (3) to develop a modified data interpretation method that uses a type-curve approach to

produce more accurate prediction of retardation from push-pull tests.

2. Governing Equations

[4] The mathematical expressions that describe one-dimensional radial flow and transport of a solute about a well in a homogenous, confined aquifer are [Hoopes and Harleman, 1967]

$$R \frac{\partial C}{\partial t} = \alpha_L \left| \frac{A}{r} \right| \frac{\partial^2 C}{\partial r^2} - \frac{A}{r} \frac{\partial C}{\partial r} \quad (1)$$

$$A = \frac{Q}{2\pi b \theta}, \quad (2)$$

where t is time [T], r is the radial distance [L], Q is the pumping rate [L^3/T], b is the aquifer thickness [L], θ is the aquifer porosity [], C is the solute concentration [M/L^3], α_L is longitudinal dispersivity [L], and R is the solute retardation factor []. Note that in a push-pull test, the flow field around the well is initially divergent ($Q > 0$) and then convergent ($Q < 0$).

[5] The nondimensional form of (1) and (2) can be written as

$$\frac{\partial c}{\partial v} = \frac{\varepsilon}{\rho} \frac{\partial^2 c}{\partial \rho^2} - \frac{1}{2\rho} \frac{\partial c}{\partial \rho}, \quad (3)$$

where the four dimensionless terms relate to (1) the dimensionless concentration, $c = C/C_0$; (2) the dimensionless extracted volume (or dimensionless time), $v = V/V_{inj} =$

t/t_{inj} , where $V_{inj} = Q t_{inj}$; (3) the dimensionless radial distance, $\rho = r/r_w$; and (4) the dimensionless ratio ε , defined as

$$\varepsilon = \frac{\alpha_L}{2r_{max}}, \quad (4)$$

where r_{max} is the invasion radius [L] of the injected solute, equal to the frontal position in the case of pure advection. The retardation factor R is linked to the maximum invasion radius r_{max} through the relationship (assuming a negligible well radius)

$$r_{max} = \sqrt{\frac{Qt_{inj}}{\pi b \theta R}} \quad (5)$$

[6] In the case of a conservative and an adsorbing species, the dimensionless term ε of both species can be related through

$$\varepsilon = \varepsilon_1 \sqrt{R}, \quad (6)$$

where ε_1 refers to the nonadsorbing ($R = 1$) species and ε refers to the adsorbing species. From the above it is apparent that the sorption push-pull tracer breakthrough curves can be parameterized on the value of ε alone.

3. Discussion of Existing Interpretation Models

[7] *Schroth et al.* [2001] demonstrated that the retardation factor can be estimated from conservative and reactive tracer push-pull test breakthrough curves using a two-step procedure that uses the approximate analytical solution of the radial dispersion problem developed by *Gelhar and Collins* [1971]:

$$\frac{C}{C_0} = \frac{1}{2} \operatorname{erfc} \left\{ \left(\frac{V}{V_{inj}} - 1 \right) / \left[\frac{16}{3} \frac{\alpha_L}{r_{max}} \left(2 - \left| 1 - \frac{V}{V_{inj}} \right|^{1/2} \left(1 - \frac{V}{V_{inj}} \right) \right) \right]^{1/2} \right\}, \quad (7)$$

where erfc is the complementary error function.

[8] In the method proposed by *Schroth et al.* [2001], first the aquifer dispersivity α_L is estimated by applying (7) to create a breakthrough curve that matches the nonreactive tracer ($R = 1$) field data. Substituting for the known value of α_L in (7) and considering the relationship in (5), the model fitting is repeated for the adsorbing tracer until an estimate of R is obtained. The limitation of this interpretation method is that the approximate analytical solution of *Gelhar and Collins* [1971] is only accurate when $\varepsilon^{1/2} \ll 1$ [*Gelhar and Collins*, 1971] outside of which errors arise in the dispersivity estimate, which ultimately manifest themselves in the estimation of R . A reasonable upper limit to ε is therefore $\varepsilon \ll 0.01$ ($\varepsilon^{1/2} = 0.1 \ll 1$).

4. Methodology

[9] In order to investigate the interaction that may exist between ε and R , we studied a series of six base-case push-pull scenarios for which ε_1 values ranged from 0.0054 to 0.25. For each base-case we looked at reactive solutes with

retardation factors of 5 and 20. Details of the base-case scenarios are provided in Table 1. We studied parameter sensitivity from the conservative and adsorbing tracer breakthrough curves of each scenario using a numerical push-pull model, followed by the approximate analytical *Gelhar and Collins* [1971] model to serve as a comparison.

4.1. General Forward (Numerical) Model

[10] For each of the 12 combined ε_1 and R scenarios, a conservative ($R = 1$) and a reactive tracer breakthrough curve were generated using a numerical finite difference model to solve (1) with the following initial and boundary conditions:

$$C(r, t = 0) = 0 \quad \text{for } r > r_w \quad (8)$$

$$C(r_w, t) = C_0 \quad \text{for } 0 < t < t_{inj} \quad (9)$$

$$\frac{\partial C(r_w, t)}{\partial r} = 0 \quad \text{for } t_{inj} < t \quad (10)$$

$$C(r \rightarrow \infty, t) \rightarrow 0 \quad \text{for } t > 0 \quad (11)$$

where r_w is the well radius.

[11] The performance of the numerical code was assessed against the analytical solution of radial dispersion in a diverging flow field provided by *Hsieh* [1986] and with tracer breakthrough curves published by *Schroth et al.* [2001] and generated using the STOMP code. In both cases, our model produced results indistinguishable (<0.1% error) from those in the literature.

4.2. Model Inversion

[12] For each set of simulated conservative and adsorbing tracer breakthrough curves an automated nonlinear least squares, Newton-Raphson root-finding technique was used to solve for α_L , R . The inversion procedure was performed using both the numerical finite difference code and the analytical *Gelhar and Collins* [1971] solution as forward predictive models. Reactive and conservative tracer breakthrough curve data were assessed simultaneously, and α_L and R were built into a single sum-of-squares error objective function. Parameter optimization threshold limits were the same for all cases. Once the Newton-Raphson method reached convergence, an approximate confidence region was mapped in the (α_L, R) parameter space about the final optimized parameter set $(\hat{\alpha}_L, \hat{R})$.

4.3. Confidence Regions

[13] Following *Draper and Smith* [1998, p. 156], under the assumption of independent Gaussian errors on the data, an approximate $100(1 - \beta)\%$ confidence contour (β is an arbitrary confidence level and in this study was taken to equal 5%) was computed from

$$S(\alpha_L, R) = S(\hat{\alpha}_L, \hat{R}) \left\{ 1 + \frac{2}{n_1 + n_R - 2} F(2, n_1 + n_R - 2, 1 - \beta) \right\}, \quad (12)$$

where S is the sum-of-squares error objective function and n is the number of observation points on the breakthrough

Table 1. Summary of Errors in Parameter Estimates and Parameter Sensitivity Indices for the Six Studied Base-Case Scenarios When $R = 5$ and $R = 20$ and When No-Error and 2% Random Gaussian Error Had Been Added to the Tracer Breakthrough Curve Data^a

Simulated Base Case		Numerical Finite Difference Forward Model										Gelhar and Collins [1971] Forward Model											
Number	ε_1	α_L, m	R	Inversion From No Error					Inversion From 2% Error					Inversion From No Error					Inversion From 2% Error				
				$100\alpha'_L, \%$	$100R', \%$	m	M	$\Delta\alpha'_L$	$\Delta R'$	$100\alpha'_L, \%$	$100R', \%$	M	$\Delta\alpha'_L$	$\Delta R'$	$100\alpha'_L, \%$	$100R', \%$	m	$\Delta\alpha'_L$	$\Delta R'$	$100\alpha'_L, \%$	$100R', \%$	m	$\Delta\alpha'_L$
1	0.0054	0.01	5	-0.20	-0.03	-2.00	2.00	8.33	-2.04	0.30	0.83	1.00	1.00	7.04	-2.03	0.27	0.57	4.00	6.12	-2.07	0.34	0.76	0.76
	0.0054	0.01	20	0.04	-0.18	-1.97	1.80	12.86	-1.85	0.30	0.79	0.40	0.40	-10.52	-1.99	0.24	0.57	2.70	2.68	-1.94	0.28	0.73	0.73
2	0.01	0.018	5	-0.03	-0.07	-2.01	1.67	11.98	-2.08	0.25	0.73	-1.11	-1.11	-9.46	-2.06	0.23	0.55	0.56	3.42	-2.08	0.32	0.87	0.87
	0.01	0.018	20	0.00	-0.28	-1.97	0.94	9.10	-1.96	0.26	0.70	-2.78	-2.78	-18.08	-1.98	0.32	0.66	2.78	-20.48	-2.25	0.40	0.82	0.82
3	0.025	0.046	5	0.00	-0.07	-2.03	2.17	2.71	-2.06	0.22	0.59	-7.39	-7.39	-21.68	-2.12	0.34	0.77	-5.00	-20.48	-2.25	0.38	0.84	0.84
	0.025	0.046	20	-0.04	-0.22	-1.99	1.96	-4.63	-2.02	0.24	0.68	-7.39	-7.39	-46.74	-2.17	0.42	0.63	-5.65	-48.19	-2.14	0.46	0.64	0.64
4	0.05	0.092	5	0.00	-0.06	-2.05	1.82	-4.20	-2.06	0.22	0.62	-16.52	-16.52	-36.03	-2.18	0.37	0.81	-14.83	-38.70	-2.12	0.38	0.81	0.81
	0.05	0.092	20	0.00	-0.14	-1.98	1.71	-8.45	-2.00	0.21	0.67	-16.52	-16.52	-64.81	-2.22	0.42	0.50	-15.00	-66.90	-2.10	0.44	0.48	0.48
5	0.1	0.185	5	0.00	-0.04	-2.06	0.86	-6.95	-2.16	0.23	0.73	-30.92	-30.92	-50.67	-2.21	0.37	0.78	-29.78	-53.75	-2.24	0.38	0.71	0.71
	0.1	0.185	20	-0.05	-0.05	-1.88	0.70	-11.80	-2.03	0.22	0.89	-31.03	-31.03	-78.10	-2.11	0.38	0.37	-30.22	-79.39	-2.20	0.40	0.35	0.35
6	0.25	0.462	5	-0.02	-0.02	-2.10	-0.11	-12.92	-2.34	0.33	1.12	-54.68	-54.68	-64.52	-1.99	0.29	0.68	-54.16	-66.70	-1.95	0.30	0.63	0.63
	0.25	0.462	20	-0.04	0.09	-1.58	-0.50	-19.14	-2.14	0.32	1.44	-54.70	-54.70	-87.50	-2.65	0.30	0.27	-54.16	-88.37	-2.28	0.31	0.25	0.25

^aParameters and indices are explained in the text. Constant base-case parameters were $Q = 1.5624 \times 10^{-2} \text{ m}^3 \text{ h}^{-1}$, $t_{inj} = 12$ hours, $\theta = 0.35$, $\tau_w = 0.025$ m, and $b = 0.2$ m.

curve. Subscripts 1 and R denote the conservative tracer data and adsorbing tracer data, respectively. $F(\)$ is the Fisher distribution function. Note that the confidence regions developed using this approach are true in their shape but only approximate in their confidence level.

4.4. Sensitivity Analysis

[14] In order to assess the sensitivity of the model interpretation methods to measurement errors borne in the tracer breakthrough curve data, 0.5% and 2% random Gaussian error were applied to the default conservative and adsorbing tracer breakthrough curve data of the 12 scenarios. The parameter estimation and confidence-region plotting were repeated for these 24 additional scenarios, and results were compared with those from the default case in which no error was assumed.

4.5. Model Efficiency and Parameter Sensitivity Indices

[15] To assess parameter sensitivity, α_L and R were normalized with respect to the true respective parameter values α_L^* , R^* (i.e., those used to numerically generate the no-error tracer breakthrough curves), to provide α'_L and R' . The accuracy of the push-pull interpretation methods (i.e., fully numerical solution or solution using the analytical Gelhar and Collins [1971] model) was evaluated by considering the percentage error in the optimized parameter estimations of α_L and R (equivalent to $100\hat{\alpha}'_L$, $100\hat{R}'$). A measure of correlation between dispersivity and retardation was evaluated from the slope m of a linear-regression fit to the 95% confidence regions mapped in the parameter space α'_L , R' . A value of $|m| = 1$ indicates perfect correlation between the parameters, and as $|m| \rightarrow \infty$ or $|m| \rightarrow 0$ there is decreasing dependence of the parameters on each other. The indices $\Delta\alpha'_L$ and $\Delta R'$, which were calculated as the range between the minimum and maximum values of the approximate 95% confidence limits of an individual parameter, were used to highlight the relative sensitivity of each of the studied parameters.

5. Results

5.1. Parameter Sensitivity

[16] The results of the parameter estimates inverted using the numerical radial flow model and complementary approximate 95% confidence contour regions for six of the 12 base-case scenarios including 0.5% and 2% error assessments are shown in Figure 1. Sensitivity indices for all the scenarios are reported in Table 1. Confidence regions for the no-error case are not shown because they are extremely small ($S(\alpha_L, R) < 1 \times 10^{-6}$). It is apparent from Figure 1 that there is a positive, monotonic relationship between error in the breakthrough curve data and the final parameter estimate. This is not surprising since the breakthrough curves were originally generated with the same numerical model that was used in the inversion.

[17] The elliptic shape and negative slope of the confidence regions indicate that α_L and R are near-linearly, negatively correlated. The magnitude of the correlation index m for all the simulated confidence regions ranges $1.58 < |m| < 2.34$ and demonstrates that there is a dependence between α_L and R . Although m values are relatively indifferent for the simulated cases of low retardation ($R = 5$)

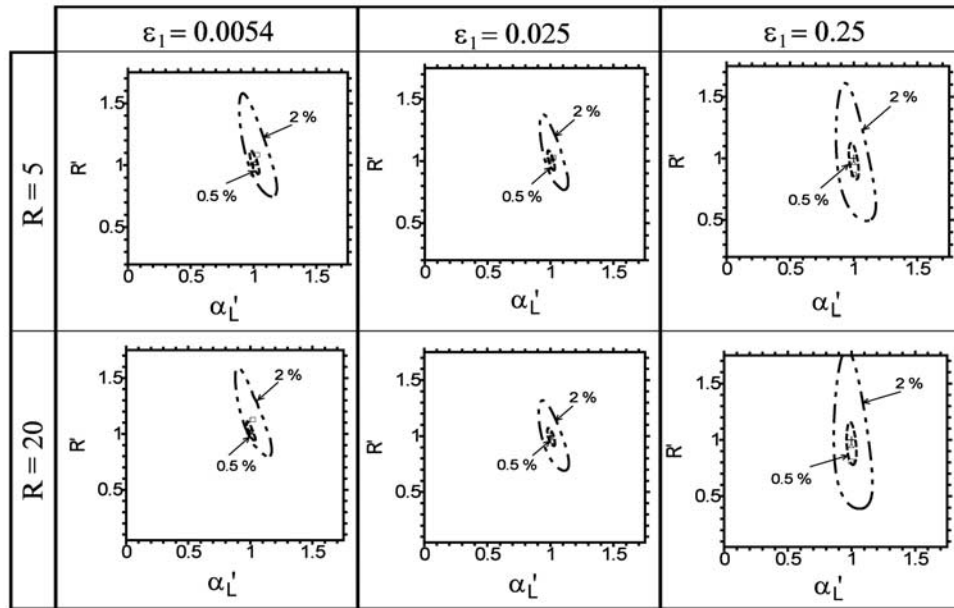


Figure 1. Confidence regions for the estimated dispersivity α_L and retardation factor R parameter values for three of the six studied base cases. Parameter estimates were obtained using an automated Newton-Raphson technique using the radial finite difference model. Parameter values in the figures are plotted as relative values (α'_L, R'), normalized with respect to the true (simulated) parameter values (α^*_L, R^*). Plus signs symbolize the true parameter set; triangles and boxes symbolize the optimal parameter estimates, and the dashed and dotted curves symbolize the approximate 95% confidence regions, after inversion from data containing 0.5% and 2% random Gaussian error, respectively. Note that no error cases are not shown, since for these cases $S(\alpha_L, R) < 1 \times 10^{-6}$.

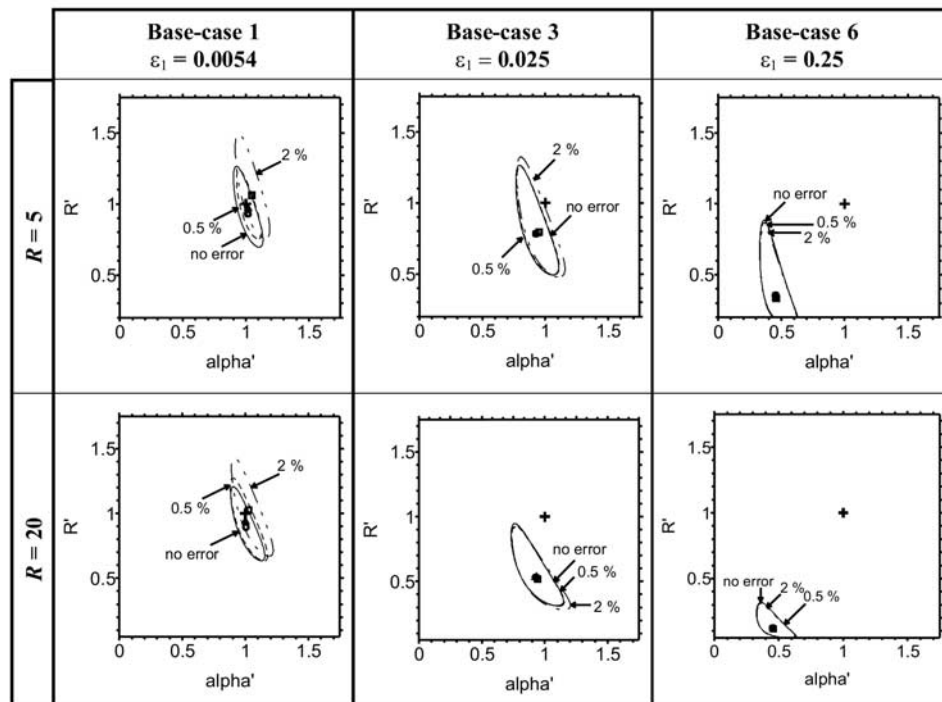


Figure 2. Approximate 95% confidence regions for the estimated dispersivity α_L and retardation factor R parameter values for three of the six studied base cases. Parameter estimates were obtained using an automated Newton-Raphson technique using the *Gelhar and Collins* [1971] model. Symbols and coding are analogous with that of Figure 1, except no error cases are included, the best estimate for which is denoted by circles and approximate 95% confidence interval by the solid curves.

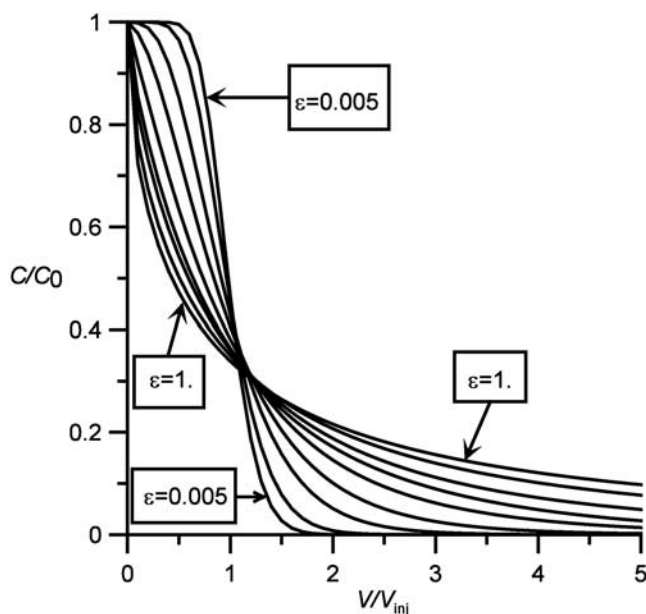


Figure 3. Dimensionless breakthrough curves for the interpretation of sorption push-pull tests. Curves are shown for $\varepsilon = 0.005, 0.01, 0.025, 0.05, 0.1, 0.175, 0.25, 1$. Numerical values for these curves are summarized in Table 2. These curves can be utilized following the procedure described in section 5.3.

($2.0 < |m| < 2.10$), at higher retardation ($R = 20$) the correlation between α_L and R is consistently greater ($1.58 < |m| < 1.99$) and grows, i.e., $|m| \rightarrow 1$, as ε increases. The measures of relative thickness of the confidence ellipses ($\Delta\alpha'_L, \Delta R'$) indicate that α_L is a well-defined parameter in the sorption push-pull model. In contrast, the data interpretation methodology is relatively insensitive to R , particularly in systems demonstrating high relative dispersivity, e.g., for base-case 6 ($\varepsilon_1 = 0.25, R = 20, \varepsilon = 1.12$), despite only 2% error in the breakthrough curve data, 19% error arose in the final R estimate $\pm 144\%$ at the approximate 95% confidence level.

[18] As a relative comparison, the results of the parameter estimates and approximate 95% confidence contour regions for the same scenarios inverted using the *Gelhar and Collins* [1971] model are shown in Figure 2 and sensitivity indices are included in Table 1. For the first three simulated base cases ($\varepsilon_1 \leq 0.025$) it is apparent that the confidence regions are of similar shape, and parameter sensitivity indices are of similar magnitude, to the inversion results obtained using the numerical radial flow model. However, in these cases, parameter estimates themselves are $< 90\%$ accurate, except for the initial case, for which $\varepsilon = 0.012$ (which is close to the value recommended by *Gelhar and Collins* [1971] for accurate application of their solution). From the results of base-case 3 upward, the effects of the approximation in the *Gelhar and Collins* [1971] solution are apparent and result in underestimations of both α_L and R . In contrast to the results of the inversions made with the numerical radial flow model, for high retardation ($R = 20$) the correlation between α_L and R decreases as ε increases. This is reflected in the decreasing ellipticity of the confidence regions in Figure 2 that indicates an increasingly nonlinear parameter relationship. Although R remains

insensitive in the $R = 5$ scenarios, when $R = 20$ the relative sensitivity of both parameters (α_L, R) decreases as ε_1 increases. Estimation of R tends to a minimal saturation level of unity, since $R < 1$ is not physically possible.

5.2. Application to Field Data

[19] The performance of the model inversion process was evaluated by applying it to estimate dispersivity and retardation parameters from the sorption push-pull field data set of *Pickens and Grisak* [1981]. These field data were similarly used by *Schroth et al.* [2001] to validate their interpretation method. The inversion was performed with the finite difference and approximate analytical push-pull models to enable a comparison to be made.

[20] Using the inversion process with our numerical finite difference scheme, respective best estimates for α_L and R of 0.063 m and 13.24 were obtained for the data ($S(\hat{\alpha}_L, \hat{R}) = 0.04$ ($n = 57$)). Respective best estimates of 0.064 m and 11.44 (identical to the results of *Schroth et al.* [2001]) were computed when the *Gelhar and Collins* [1971] solution was substituted as the forward model in the inversion process ($S(\hat{\alpha}_L, \hat{R}) = 0.10$ ($n = 57$)). The numerically derived estimate of $R = 13.24$ falls within the solute retardation factor range $12.6 < R < 36.3$ measured from lab and field experiments reported by *Pickens et al.* [1981]. From the resulting parameter estimates, values of $\varepsilon_1 = 0.013$ and $\varepsilon = 0.046$ were evaluated, the latter being above the limit for accurate application of the *Gelhar and Collins* [1971] solution ($\varepsilon^{1/2} \ll 1$). This would explain the relatively small but measurable difference in R estimates between our approach and the method proposed by *Schroth et al.* [2001]. It is useful to note that the errors in the tracer breakthrough curve data of *Pickens and Grisak* [1981] measured against the numerically simulated data were approximately 2.7% and almost normally distributed. Thus the Gaussian error that we applied to the breakthrough curve data of our base-case scenarios is reasonably representative of that encountered in the field.

5.3. Simplified Interpretation Method

[21] On the basis that in nondimensional form, sorption push-pull tracer breakthrough curves can be parameterized on the value of ε alone, a simplified sorption interpretation procedure can be developed that overcomes the limitations of the *Gelhar and Collins* [1971] approximation that consequently limits the applicability of the interpretation method proposed by *Schroth et al.* [2001]. Figure 3 contains a set of dimensionless tracer breakthrough curves generated using our numerical radial-flow model for the range $0.005 < \varepsilon < 1.0$. For all cases a negligible well radius has been assumed and injection and abstraction flow rates were equal. Note that all breakthrough curves contain more solute mass than from a simple $C_0 \times V_{inj}$ calculation. This is the result of a non-negligible dispersion component at the well face that causes more solute to be flushed into the aquifer than by pure advection, as well known from the literature [e.g., *Chen, 1987; P. A. Hsieh, personal communication, 2002*]. This effect is more evident for large ε values, since ε can be envisaged as a ratio between dispersive and advective components of the injection process.

[22] The interpretation procedure is as follows:

[23] 1. Plot the conservative tracer and the adsorbing solute breakthrough curves on a C/C_0 versus V/V_{inj} scale.

Table 2. Numerical Values for the Dimensionless Breakthrough Curves Shown in Figure 3 for the Interpretation of a Sorption Push-Pull Test

V/V _{inj}	ε = 0.005	ε = 0.01	ε = 0.025	ε = 0.05	ε = 0.1	ε = 0.175	ε = 0.25	ε = 0.5	ε = 1
0	1	1	1	1	1	1	1	1	1
0.1	1	0.999999	0.998463	0.97842	0.918156	0.854315	0.822414	0.767336	0.723964
0.2	1	0.999917	0.988912	0.937126	0.84401	0.766226	0.730779	0.673218	0.630237
0.3	0.999992	0.998583	0.963419	0.879665	0.770403	0.691167	0.657342	0.603762	0.564526
0.4	0.999669	0.990673	0.917705	0.811716	0.699876	0.625668	0.595589	0.548204	0.51357
0.5	0.995905	0.965208	0.852713	0.738624	0.633887	0.568045	0.542556	0.50204	0.472102
0.6	0.976144	0.910615	0.773226	0.664643	0.57309	0.517114	0.496432	0.462784	0.437345
0.7	0.9175	0.822711	0.685621	0.592808	0.517645	0.471937	0.455952	0.428858	0.407614
0.8	0.803496	0.707931	0.59605	0.525083	0.467421	0.431735	0.420173	0.39918	0.381795
0.9	0.642923	0.579949	0.509443	0.462592	0.422127	0.39585	0.388362	0.372967	0.359104
1.0	0.466869	0.4536	0.429185	0.405843	0.381395	0.363723	0.359935	0.349632	0.338969
1.1	0.308511	0.340218	0.357217	0.354926	0.344827	0.334878	0.334417	0.328707	0.320956
1.2	0.186958	0.245914	0.294326	0.309657	0.312028	0.308905	0.311418	0.309845	0.304732
1.3	0.104904	0.172128	0.240481	0.269689	0.282617	0.285455	0.290613	0.29275	0.29003
1.4	0.055038	0.117194	0.19513	0.234589	0.256243	0.264225	0.271729	0.27719	0.27664
1.5	0.027248	0.077925	0.157432	0.203891	0.232581	0.244957	0.254536	0.262967	0.264387
1.6	0.012833	0.050779	0.126428	0.177125	0.211339	0.227424	0.238838	0.249919	0.253128
1.7	0.005792	0.032528	0.101147	0.153841	0.192253	0.211434	0.224466	0.237909	0.242744
1.8	0.00252	0.020536	0.080677	0.13362	0.175089	0.196816	0.211276	0.226821	0.233135
1.9	0.001063	0.012807	0.064196	0.11608	0.159637	0.183424	0.199142	0.216555	0.224216
2.0	0.000437	0.007905	0.050986	0.100877	0.14571	0.171129	0.187956	0.207026	0.215913
2.1	0.000175	0.004837	0.040438	0.087707	0.133144	0.159818	0.177622	0.19816	0.208164
2.2	6.91E-05 ^a	0.002938	0.032039	0.0763	0.121792	0.149394	0.168057	0.189892	0.200915
2.3	2.68E-05	0.001774	0.025367	0.066419	0.111525	0.13977	0.159188	0.182167	0.194118
2.4	1.02E-05	0.001066	0.020076	0.057859	0.102228	0.130869	0.150948	0.174933	0.187733
2.5	3.87E-06	0.000638	0.015886	0.05044	0.093799	0.122624	0.143283	0.168149	0.181722
2.6	1.45E-06	0.000381	0.01257	0.044009	0.086147	0.114975	0.136139	0.161774	0.176053
2.7	5.38E-07	0.000226	0.009949	0.038429	0.079194	0.107869	0.129472	0.155775	0.170698
2.8	1.98E-07	0.000134	0.007877	0.033586	0.072867	0.10126	0.123242	0.150121	0.165632
2.9	7.28E-08	7.98E-05	0.00624	0.029379	0.067104	0.095105	0.117411	0.144785	0.160831
3.0	2.66E-08	4.73E-05	0.004945	0.025722	0.061848	0.089366	0.111948	0.139741	0.156276
3.1	9.7E-09	2.8E-05	0.003922	0.02254	0.05705	0.084009	0.106822	0.134967	0.151948
3.2	3.53E-09	1.66E-05	0.003113	0.01977	0.052665	0.079005	0.102007	0.130444	0.14783
3.3	1.28E-09	9.81E-06	0.002473	0.017356	0.048652	0.074326	0.09748	0.126154	0.143908
3.4	4.64E-10	5.81E-06	0.001966	0.015251	0.044977	0.069946	0.093218	0.122079	0.140168
3.5	1.68E-10	3.44E-06	0.001565	0.013413	0.041608	0.065845	0.089202	0.118205	0.136597
3.6	6.1E-11	2.04E-06	0.001247	0.011807	0.038515	0.062001	0.085414	0.114518	0.133186
3.7	2.21E-11	1.21E-06	0.000994	0.010403	0.035675	0.058396	0.081838	0.111006	0.129922
3.8	8.04E-12	7.21E-07	0.000793	0.009174	0.033063	0.055013	0.078458	0.107658	0.126798
3.9	2.92E-12	4.29E-07	0.000634	0.008097	0.03066	0.051837	0.075261	0.104462	0.123803
4.0	1.06E-12	2.56E-07	0.000507	0.007153	0.028447	0.048854	0.072234	0.10141	0.120931
4.1	3.88E-13	1.53E-07	0.000406	0.006324	0.026406	0.04605	0.069366	0.098493	0.118175
4.2	1.42E-13	9.14E-08	0.000326	0.005596	0.024524	0.043413	0.066647	0.095701	0.115526
4.3	5.21E-14	5.48E-08	0.000261	0.004956	0.022786	0.040934	0.064067	0.093029	0.11298
4.4	1.92E-14	3.29E-08	0.00021	0.004392	0.021181	0.038601	0.061617	0.090469	0.110531
4.5	7.06E-15	1.98E-08	0.000169	0.003896	0.019696	0.036405	0.059288	0.088014	0.108172
4.6	2.61E-15	1.19E-08	0.000136	0.003459	0.018323	0.034338	0.057074	0.085659	0.1059
4.7	9.68E-16	7.18E-09	0.00011	0.003073	0.017052	0.032391	0.054967	0.083398	0.10371
4.8	3.6E-16	4.34E-09	8.85E-05	0.002732	0.015874	0.030558	0.05296	0.081226	0.101597
4.9	1.34E-16	2.63E-09	7.15E-05	0.002431	0.014783	0.02883	0.051048	0.079138	0.099558
5.0	5.03E-17	1.6E-09	5.78E-05	0.002165	0.01377	0.027202	0.049225	0.07713	0.097588

^aRead as 6.91 × 10⁻⁵.

[24] 2. Find the best curve of the set in Figure 3 that matches the field data for the conservative tracer (no shift is needed), and identify the corresponding value for ε₁.

[25] 3. From ε₁ we can calculate the longitudinal dispersivity explicitly rearranging equation (4):

$$\alpha_L = 2\varepsilon_1 \sqrt{\frac{Qt_{inj}}{\pi b \theta}} \tag{13}$$

[26] 4. Find the best curve of the set in Figure 3 that matches the field data for the adsorbing solute in the same way done for the conservative tracer in step 2, and identify the corresponding value of ε.

[27] 5. From ε, and knowing ε₁ from step 2, we can calculate the retardation factor rearranging equation (6):

$$R = \left(\frac{\varepsilon}{\varepsilon_1}\right)^2 \tag{14}$$

Table 2 provides the values necessary to reproduce Figure 3 to be used as a chart for this procedure.

6. Discussion and Conclusions

[28] Using an automated nonlinear least squares inversion procedure with an approximate confidence region algorithm, we have been able to analyze the interpretation of

instantaneous linear sorption push-pull tests. From our work we have concluded the following:

[29] 1. A sensitivity analysis of the two governing parameters of sorption push-pull tests, α_L and R , has shown that their estimates are negatively correlated to a certain degree, and this correlation is more pronounced for smaller values of ε . It has also been shown that α_L is well defined in the push-pull test interpretation methodology, whereas R is a relatively insensitive parameter.

[30] 2. When analyzed in the context of confidence regions, α_L can be estimated very precisely, even when reasonable realistic errors are implicit to the breakthrough curve data. In contrast, R estimates show a very wide range of uncertainty that increases as ε increases, i.e., as dispersion becomes increasingly important over the distance traveled by the solute. The conclusion is that errors in the breakthrough curve can propagate to generate fairly large errors in the estimates of R .

[31] 3. The problems of using the *Gelhar and Collins* [1971] as a forward model to interpret sorption push-pull test data have been clearly demonstrated. From our sensitivity analysis performed using the *Gelhar and Collins* [1971] model, we notice that the true parameter values are not even within the approximate 95% confidence regions of the optimized estimates $\hat{\alpha}_L$, \hat{R} when ε and ε_1 are greater than 0.06. The actual optimized parameter estimates in these cases are as much as -7.6% (α_L) and -21.7% (R) in error. Note that *Gelhar and Collins* [1971] claimed that their method yielded usable dispersivity estimates for ε as high as 0.07, which is consistent with our findings. Unfortunately, a good estimation of R with the same approach requires that ε be substantially smaller. In one case recorded by *Schroth et al.* [2001] in their Table 1 (high $\alpha_L = 10$ cm, $R = 10$), $<10\%$ error in R estimate was achieved using their interpretation method (that incorporates the *Gelhar and Collins* [1971] model), when ε was as high as 0.17 (and $\varepsilon_1 = 0.05$). When we interpreted the same case using our automated inversion process, we derived -16.4% and -38% errors in α_L and R , respectively ($S(\hat{\alpha}_L, \hat{R}) = 0.31$ ($n = 48$)). We interpret such discrepancies between *Schroth et al.*'s [2001] and our findings as a symptom that their approximate fitting of the

approximate *Gelhar and Collins* [1971] solution may, at times, lead to a better solution. However, there does not seem to be any guarantee that this is generally the case. If using the *Gelhar and Collins* [1971] model to invert sorption push-pull test data with a single objective function, then our results suggest it would be prudent to do so only if ε and $\varepsilon_1 < 0.02$, as above this value we observed $>10\%$ error in \hat{R} . This in itself presents a paradox, for it is generally not possible to evaluate ε a priori.

[32] 4. The simplified type-curve approach that we have devised for interpreting instantaneous linear sorption in push-pull tests performed in confined aquifers should help overcome this hurdle. The method treats push-pull data in a nondimensional form and is not constrained mathematically by the value of ε .

References

- Chen, C. S. (1987), Analytical solutions for radial dispersion with Cauchy boundary at injection well, *Water Resour. Res.*, 23(7), 1217–1224.
- Draper, N. R., and H. Smith (1998), *Applied Regression Analysis*, 3rd ed., John Wiley, Hoboken, N. J.
- Gelhar, L. W., and M. A. Collins (1971), General analysis of longitudinal dispersion in nonuniform flow, *Water Resour. Res.*, 7(6), 1511–1521.
- Hoopes, J. A., and D. R. Harleman (1967), Dispersion in radial flow from a recharge well, *J. Geophys. Res.*, 72(14), 3595–3607.
- Hsieh, P. A. (1986), A new formula for the analytical solution of the radial dispersion problem, *Water Resour. Res.*, 22(11), 1597–1605.
- Pickens, J. F., and G. E. Grisak (1981), Scale-dependent dispersion in a stratified granular aquifer, *Water Resour. Res.*, 17(4), 1191–1211.
- Pickens, J. F., R. E. Jackson, K. J. Inch, and W. F. Merritt (1981), Measurement of distribution coefficients using a radial injection dual-tracer test, *Water Resour. Res.*, 17(3), 529–544.
- Schroth, M. H., J. D. Istok, and R. Haggerty (2001), In-situ evaluation of solute retardation using single-well push-pull tests, *Adv. Water Resour.*, 24, 105–117.

L. F. Burbery, Department of Environmental Science, Lancaster University, Bailrigg, Lancaster, LA1 4YQ, UK.

G. Cassiani, Dipartimento di Scienze Geologiche e Geotecnologie, Università di Milano-Bicocca, Piazza della Scienza 4, 20125 Milano, Italy. (giorgio.cassiani@unimib.it)

M. Giustiniani, Dipartimento di Ingegneria Civile ed Ambientale, Sezione Georisorse e Ambiente, Università di Trieste, Via Valerio 10, 34100 Trieste, Italy.